Polymer Chemistry

Accepted Manuscript

ROYAL SOCIETY OF CHEMISTRY

www.rsc.org/polymers

Polymer Chemistry

RSCPublishing

ARTICLE

Synthesis of Core Cross-linked Star Polystyrene with Functional End Groups and the Self-assemblies Templated by Breath Figures

Cite this: DOI: 10.1039/x0xx00000x

Received ooth January 2012,
Accepted ooth January 2012

DOI: 10.1039/x0xx00000x

www.rsc.org/

Liang-Wei Zhu, Wu Yang, Ling-Shu Wan* and Zhi-Kang Xu

In this paper, we report the synthesis of core cross-linked star (CCS) polymers with functional end groups for self-assembled films, which show monolayer, bilayer, or multilayer structure, depending on arm numbers, arm length, and the end groups. The stars were synthesized via the "arm-first" method using a linear polystyrene as an atom transfer radical polymerization (ATRP) macroinitiator that is end-capped with a hydrolysable cyclic lactone end group. The relatively hydrophobic cyclic group can be converted into hydrophilic neutralized carboxyl and hydroxyl groups via alkaline hydrolysis and acidification processes. The polymers were characterized by gel permeation chromatography (GPC), Fourier transform infrared spectroscopy (FTIR), and nuclear magnetic resonance spectroscopy (NMR). The conversion of the macroinitiators was evaluated by fitting the GPC curves. We found that the star polymers are easier to form ordered honeycomb films than the corresponding linear analogue. Moreover, the end groups of the stars show obvious impact on the film surface structures only at relatively low concentration. More importantly, stars with lower arm numbers or longer arms tend to form bilayer or multilayer structured films. On the other hand, stars with hydrophilic end groups are much easier to form bilayer or multilayer structured films. Considering the importance of mono- or multilayer structures of honeycomb films in various fields such as separation membranes, templating materials, and optical materials, these results will be valuable in tailoring film-forming materials toward films with designed structures.

Introduction

The breath figure method, which is inspired by the formation of fog on cold surfaces, has been commonly used to fabricate hexagonally-patterned honeycomb films.[1] In the breath figure process, water droplets condense onto a polymer solution surface that is cast on a substrate under humid conditions. Driven by the Marangoni convection and thermocapillary effect, the condensed water droplets arrange into a hexagonally close-packed structure. These water droplets serve as a sacrificial template and ultimately leave an ordered porous honeycomb film after thoroughly evaporation of the solvent and water.[2-11] Thanks to the cost efficiency and simple operation, the breath figure method has shown great potential applications in various fields, including photoelectronics, sensors, catalysis, microcontainers, superhydrophobic and adhesive surfaces, biomaterials, and separation membranes.[12-40]

It is well known that the properties of honeycomb films are closely related to or even mainly determined by the film structures, which, in turn, are largely dependent on the topology and chemical composition of the film-forming materials. Star polymer is the first class material that has been used for preparing honeycomb films by the breath figure method, which is believed to be a good candidate to form highly ordered structures because it is much easier than the corresponding linear polymers to precipitate at the solution/water interface to stabilize the water droplets.[41-48] Notably, the arm number, arm length, and glass transition temperature (T_g) of a star polymer display a dramatic influence on the structures of the resultant honeycomb films. For instance, Stenzel et al. proposed that the pore diameter of honeycomb films increases with the molecular weight of arms while keeping the arm number constant, and decreases with the arm number by maintaining an equivalent star molecular weight.[42] Star polymer is also one of the most often used polymers to prepare three-dimensional (3D) honeycomb films on non-planar substrates. A series of star polymers have been detailedly studied by Qiao's group for the formation of non-cracking 3D structures on non-planar substrates. They first evaluated the effects of T_g of star polymers on the non-cracking property.[44-45] In a later publication, the principle is extended and the authors suggested that the Young's modulus (E) should be a more important factor than T_g.[48]

The effects of polar end groups or blocks on the film morphologies have also attracted increased attention in recent years. In the early times, Stenzel et al. found that the pore diameter of honeycomb films decreases from 750 nm to 450 nm when converting the end group of a five-arm star polymer,

which was prepared using a multi-functional initiator, from bromide to pentadecafluoro-1-octanolate.[42] Later, Qiao et al. discovered that the pore diameter, regularity and pore shape can be significantly influenced by changing the end groups (acetonide, hydroxyl, and pentadecafluorooctanoyl groups) of core cross-linked star (CCS) polymers.[46] We synthesized a four-arm porphyrin-cored star polymer using the "core-first" strategy and then introduced a very short hydrophilic block to form an end-functionalized star polystyrene, TPP(PS-*b*-PHEMA)$_4$.[49] Interestingly, we found that the honeycomb films change from monolayer to multilayer after introducing the polar block. However, it is hard to control and measure the exact number of polar blocks in the star block copolymer. Recently, we developed a convenient strategy to functionalize polymer chain-end on the basis of a hydrolysable cyclic lactone atom transform radical polymerization (ATRP) initiator.[50]

In this work, a series of CCS polystyrenes with definite end groups were synthesized via the "arm-first" method using linear polystyrenes, which were initiated by the hydrolysable ATRP initiator (**Scheme 1**). The lactone end group was converted into neutralized carboxyl and hydroxyl groups by a hydrolysis and acidification process; the latter end group (one carboxyl plus one hydroxyl) is much more hydrophilic than the former one (lactone). The end-functionalized CCS polymers with different arm length as well as different arm numbers were then utilized to fabricate honeycomb films via the breath figure method. The end groups of the CCS polymers show obvious effects on the film morphologies. This work provides a facile approach to the synthesis of CCS polymers with definite and tunable end groups that have different hydrophilicity. Furthermore, it is a comprehensive investigation on the effects of arm number, arm length, and end group of CCS polymers on the structure of honeycomb films, which show monolayer, bilayer, or multilayer structures. This work is useful in further understanding the intrinsic mechanism of the breath figure method as well as designing honeycomb films with controllable structures.

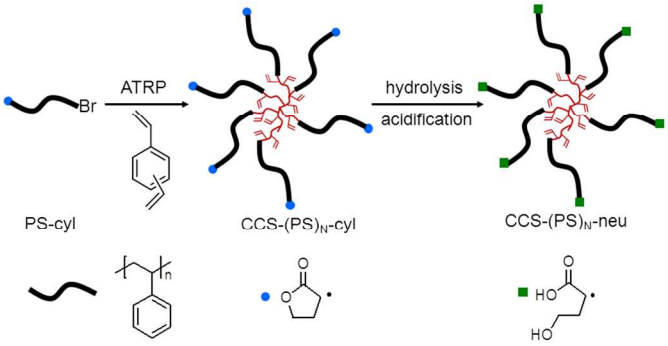

Scheme 1. Synthetic route of end-functionalized core cross-linked star (CCS) polystyrene. The core is cross-linked by divinylbenzene.

Experimental

Materials

N,N,N,N',N'-Pentamethyldiethylenetriamine (PMDETA, Aldrich) was distilled from calcium hydride and stored at room temperature in a desiccator. Styrene (St) and divinylbenzene (DVB) was obtained from Sinopharm Chemical Reagent Co. and distilled under reduced pressure before use. α-Bromo-γ-butyrolactone (**I**, 97%, Aldrich), was used as an initiator without further purification. Copper (I) bromide (CuBr) was stirred in glacial acetic acid overnight, filtered, and washed with absolute ethanol under an argon blanket. The compound was dried under reduced pressure at 60 °C overnight. Deuterated chloroform ($CDCl_3$, 99.9%) was purchased from Sigma. Poly(ethylene terephthalate) (PET) film was kindly provided by Hangzhou Tape Factory and cleaned with acetone for 2 h before use. Water used in all experiments was deionized. All other chemicals were analytical grade and used as received.

Synthesis of CCS Polystyrene with Cyclic End Group, CCS–(PS)$_N$–cyl

The subscript N in CCS–(PS)$_N$–cyl is the number of arms.The synthesis was performed based on the "arm-first" strategy. The utilized linear polystyrenes with a cyclic lactone end group, PS–cyl, have been reported in our previous work.[50] Their molecular weights are 2960, 4440, and 5950 g mol^{-1}, and the polydispersity index (PDI) is less than 1.10. The synthetic procedure of CCS polystyrene with hydrolysable five membered lactone end group is described here using $[DVB]_0/[PS–cyl]_0/[CuBr]_0/[PMEDTA]_0$ = 6/1/1/2 as a typical example. A 50 mL Schlenk flask was charged with PS–cyl (0.223 mmol), PMDETA (0.446 mmol, 92.3 μL), anisole (5 mL) and DVB (1.338 mmol, 190 μL) under a nitrogen atmosphere. The solution was degassed by three freeze–pump–thaw cycles. Then, CuBr (0.223 mmol, 32.1 mg) was added and another three freeze–pump–thaw cycles were performed. The polymerization was allowed to proceed at a preheated 110 °C oil bath. After that, the flask was quenched in liquid nitrogen to stop the polymerization. Then the reaction mixture was dissolved with a small amount of tetrahydrofuran (THF), precipitated in methanol, and filtered. The dissolution–precipitation process was repeated three times. The obtained product was dried in vacuum overnight. **Table 1** lists the details of the stars prepared with the ratios of $[DVB]_0$ to $[PS–cyl]_0$ ranging from 6 to 15, and **Table 2** shows the results of the stars prepared by changing the polymerization time. Using Gaussian fitting, we analyzed the GPC curves (**Fig. S1**). The conversion of the macroinitiator, PS-cyl, can be calculated according to the peak areas of the fitted curves.

Table 1 Results of Stars Synthesized at Different Ratios of $[DVB]_0$ to $[PS-cyl]_0$

Entry [a]	$M_{n(PS-cyl)}$ [b]	X	Time (h)	Conv. (%) [c]	$M_{n,GPC}$ [d]	PDI [d]	N_{arm} [e]
1	4440	6	13	87.1	61600	1.42	11.8
2	4440	10	5	86.4	42900	1.44	8.2
3	4440	15	4	89.9	47500	1.95	9.1

[a] Reaction conditions:$[DVB]_0/[PS-cyl]_0/[CuBr]_0/[PMEDTA]_0$ = X/1/1/2, polymerization at 110 °C in anisole. [b] The molecular weight of linear polystyrene. [c] Calculated from the integral ratio of the peak area from the GPC curves using Gaussian fitting. [d] GPC using differential refractive index detection vs. linear polystyrene standards. [e] $N_{arm} = M_{n,GPC(star)} \times arm_{wt\%}/M_{n(PS-cyl)}$.

Synthesis of CCS Polystyrene with Ionized End Group, CCS–(PS)$_N$–ion, via Hydrolysis of CCS–(PS)$_N$–cyl

In a typical hydrolysis reaction, 600 mg of CCS–(PS)$_N$–cyl in 20 mL of THF and 2 g of NaOH (50 mmol) in water (4 mL) were added into a 250 mL round-bottomed flask. The mixture

was refluxed for 24 h and then precipitated in methanol. The precipitation procedure was performed three times. The obtained product was dried in a vacuum oven overnight to achieve the final product. Please note that CCS–$(PS)_N$–ion has a hydroxyl end group (–OH) adjacent to the ionized carboxyl (–COONa).

Table 2 Results of Core Cross-linked Star Polystyrene Prepared via ATRP

entry[a]	$M_{n(PS\text{-}cyl)}$[b]	Time (h)	Conv. (%)[c]	$M_{n,GPC(star)}$[d]	PDI[d]	N_{arm}[e]
4	2960	2.75	74.8	13200	1.24	3.6
5	2960	6.00	90.2	28700	1.40	7.8
6	2960	9.50	91.7	39900	1.56	10.8
7	2960	13.00	96.6	56400	1.67	15.3
8	4440	3.00	79.2	20100	1.18	3.8
9	4440	8.34	85.6	41600	1.39	8.0
10	4440	13.00	87.1	61600	1.42	11.8
11	4440	18.00	87.4	86200	1.57	16.5
12	5950	3.50	70.9	22100	1.17	3.3
13	5950	6.50	80.1	60500	1.33	8.9
14	5950	14.00	82.5	90100	1.47	13.3
15	5950	25.00	86.9	113700	1.68	16.9

[a] Reaction conditions: $[DVB]_0/[PS\text{-}cyl]_0/[CuBr]_0/[PMEDTA]_0$ = 6/1/1/2, polymerization at 110 °C in anisole. [b] The molecular weight of linear polystyrene. [c] Calculated from the integral ratio of the peak area from the GPC curves using Gaussian fitting. [d] GPC using differential refractive index detection vs linear polystyrene standards. [e] $N_{arm} = M_{n,GPC(star)} \times arm_{wt\%}/M_{n(PS\text{-}cyl)}$.

Synthesis of CCS Polystyrene with Neutralized End Group, CCS–$(PS)_N$–neu, via Acidification of CCS–$(PS)_N$–ion

The procedure of acidification was performed as follows. CCS–$(PS)_N$–ion (200 mg) was dissolved in 11 mL of THF/methanol mixture (10/1, v/v) in a 50 mL round-bottomed flask. Then 2 mL of hydrochloric acid was added, and the reaction proceeded at ambient temperature for 1 h. The raw product was precipitated in methanol, repeated three times, and then dried in a vacuum oven overnight to achieve the final product. Please note that CCS–$(PS)_N$–neu has a hydroxyl end group (–OH) adjacent to the neutralized carboxyl (–COOH).

Formation of Self-assembled Honeycomb Films via the Breath Figure Method

The polymers were dissolved in carbon disulfide with different concentrations. An aliquot of 50 μL for each polymer solution was drop-cast onto a PET substrate placed under a 2 L/min humid airflow (25 °C and ~80% RH). Owing to the condensation of water vapor on the solution surface during the evaporation of carbon disulfide, the transparent solution turned turbid rapidly. After solidification, the film was dried at room temperature.[51]

Instruments and Measurements

Nuclear magnetic resonance (NMR) spectra were recorded on a Bruker (Advance DMX500) NMR instrument with tetramethylsilane (TMS) as the internal standard and $CDCl_3$ as the solvent at room temperature.

Fourier transform infrared (FTIR) spectra were collected on a Nicolet FTIR/Nexus 470 spectrometer. Thirty-two scans were taken for each spectrum at a nominal resolution of 1 cm^{-1}.

Molecular weight and molecular weight distribution were measured by a PL 220 gel permeation chromatography (GPC) instrument at 25 °C, which was equipped with a Waters 510 HPLC pump, three Waters Ultrastyragel columns (500, 103, and 105 Å), and a Waters 410 DRI detector. THF was used as the eluent at a flow rate of 1.0 mL/min. The calibration of the molecular weights was based on PS standards.

A field emission scanning electron microscope (FESEM, Sirion-100, FEI) was used to observe the surface morphology of films after being sputtered with gold using ion sputter JFC-1100.

Results and discussion

Synthesis and Characterization of Chain-End Functionalized Star Polystyrenes

Typically, star polymers are often synthesized via three general strategies, i.e., "coupling-onto", "core-first", and "arm-first".[52-55] Among them, the "arm-first" approach has been attracting enormous attention because of the advantages of easily regulating the arm number and precisely controlling the arm length, which benefits from the well-established controlled/"living" radical polymerizations.[56-58] The present work synthesizes CCS polystyrenes via the "arm-first" approach with a linear PS macroinitiator that has a hydrolysable lactone end group. DVB was used as the crosslinking agent, which has been confirmed by Matyjaszewski et al. as a more appropriate divinyl coupling agent for the ATRP of PS macroinitiators than other crosslinking agents such as 1,4-butanediol diacrylate (BDA) and ethylene glycol dimethacrylate (EGDMA).[52]

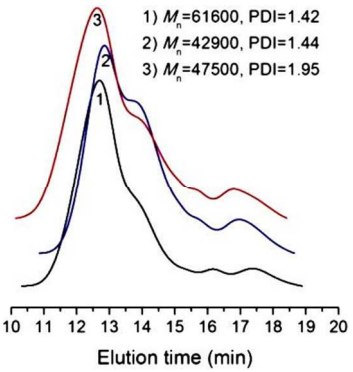

Fig. 1 GPC curves of core cross-linked star polystyrenes prepared with different ratios of $[DVB]_0$ to $[PS\text{-}cyl]_0$.

It is known that the ratio of DVB to macroinitiator exhibits a significant effect on the structure of the star polymers, including molecular weight distribution and the degree of cross-linking. Moreover, high ratio of DVB to macroinitiator may induce an insoluble gel. In order to achieve optimal conditions, effects of the ratio of $[DVB]_0$ to $[PS\text{–}cyl]_0$ were investigated first. **Table 1** lists the results of star polystyrenes prepared with the ratios of $[DVB]_0$ to $[PS\text{–}cyl]_0$ ranging from 6 to 15. Polymerization with higher DVB ratio proceeded for shorter time, leading to broader molecular weight distribution, lower molecular weights, and lower arm numbers. If the reaction time

is rationally controlled to prevent gelation, similar conversion of the macroinitiator can be achieved. From the GPC curves (**Fig. 1**), we can see that the star polystyrene prepared with $[DVB]_0/[PS–cyl]_0$ = 6 shows the faintest shoulder peak, the highest molecular weight, and the lowest PDI.

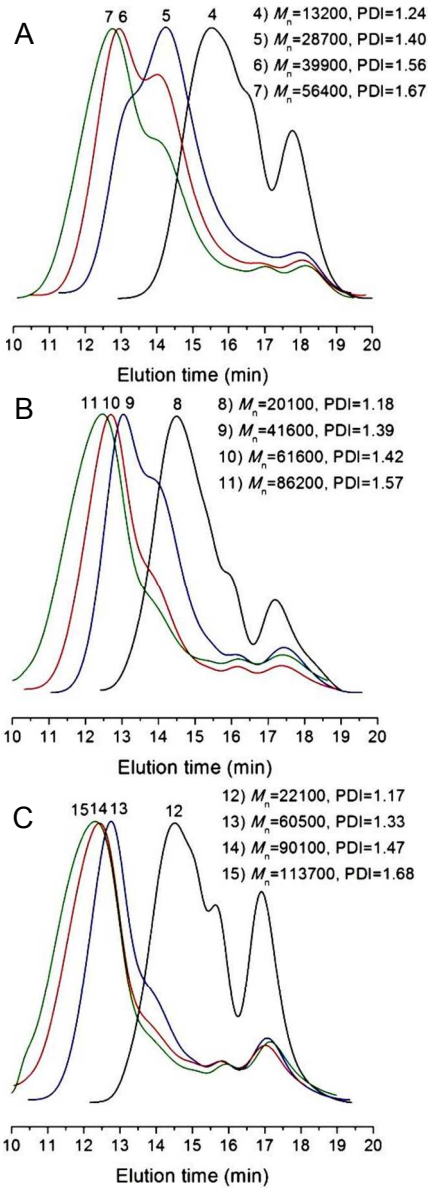

Fig. 2 GPC curves of core cross-linked star polystyrenes prepared via ATRP. The molecular weight of the arm is (A) 2960, (B) 4440 and (C) 5950 g/mol.

Table 2 shows the star polymers with gradient numbers of arms prepared by changing the reaction time. The conversion of the macroinitiators, which is calculated by fitting the GPC curves (**Fig S1**), increases remarkably at the beginning of the reaction and then levels off as the reaction proceeds. The GPC curves (**Fig. 2**) further confirm the results. A large amount of residual macroinitiator PS–cyl remains in the reaction systems when the reaction time is too short or the conversion is too low (entry 4, 8, and 12), regardless of the molecular weight of the macroinitiators. By prolonging the reaction time to more than 6 h, only about 10~20% macroinitiators remain, which may have little influence on the film formation.[42,46] Therefore, the linear polystyrene has not been separated from the CCS polymer.

Hydrolysis of the lactone end group was carried out under alkaline condition to give CCS–$(PS)_N$–ion, which was further converted into CCS–$(PS)_N$–neu through an acidification process at room temperature. These star polymers were characterized by FTIR (**Fig. 3**) and ^{1}H NMR (**Fig. 4**). As shown in the FTIR spectra, the absorption band at 1777 cm^{-1}, which is attributed to the carboxyl in the cyclic end group, disappears completely after hydrolysis (**Fig. 3A, B**). Moreover, the shoulder peaks at 1565 cm^{-1} and 1408 cm^{-1}, which are derived from sodium carboxylate, can be clearly observed although they overlapped with the peaks arising from the vibrations of the main chain of polystyrene. Unfortunately, the hydrolyzed star polymer with ionized end groups, CCS–$(PS)_N$–ion, is insoluble in common organic reagents, making it difficult to be characterized by ^{1}H NMR. The complete disappearance of the characteristic peak at 1777 cm^{-1} in the FTIR spectrum, however, is a strong support to the alkaline hydrolysis process, which is also strongly verified by our previous results about the corresponding linear polystyrene characterized by FTIR, ^{13}C and ^{1}H NMR techniques.[50] After acidification, the characteristic peak of the carbonyl group at 1777 cm^{-1} appears again, and the shoulder peaks arising from sodium carboxylate disappear (**Fig. 3C**). The ^{1}H NMR spectra of CCS–$(PS)_N$–cyl and CCS–$(PS)_N$–neu are presented in **Fig. 4**. It can be seen that, as expected, the acidification process is accompanied by both intramolecular esterification and protonation processes, which is in accordance with the results of linear polystyrene.[50]

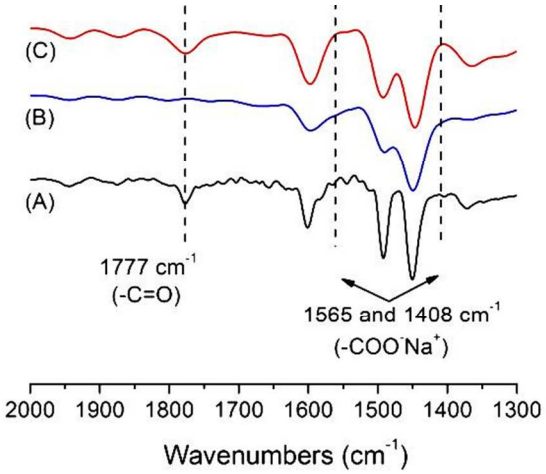

Fig. 3 FTIR spectra of (A) CCS-$(PS)_{16}$-cyl, (B) CCS-$(PS)_{16}$-ion, (C) CCS-$(PS)_{16}$-neu with $M_{n(PS)}$ = 5950 g/mol.

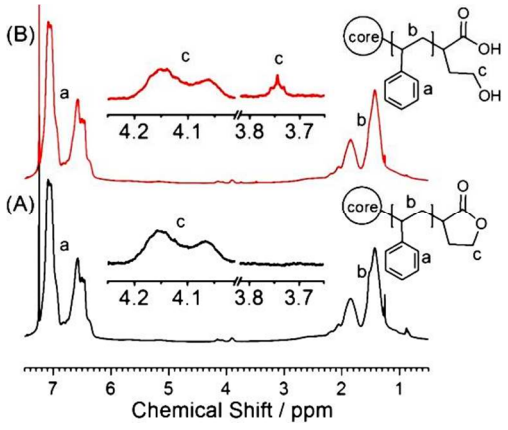

Fig. 4 ^{1}H NMR spectra of (A) CCS-$(PS)_{16}$-cyl, (B) CCS-$(PS)_{16}$-neu with $M_{n(PS)}$ = 5950 g/mol.

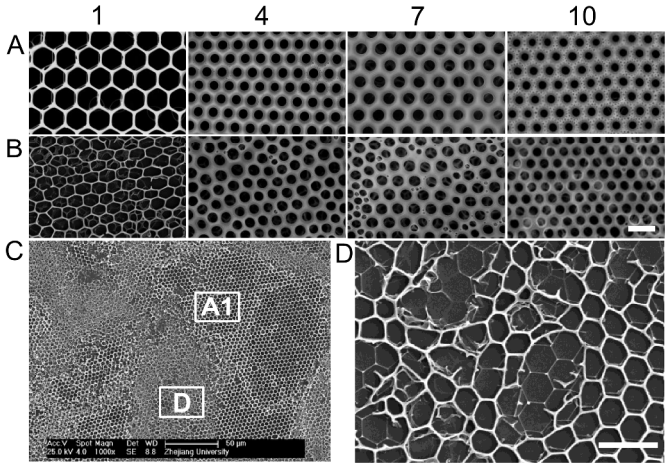

Fig. 5 SEM images of honeycomb films prepared from (A) CCS-$(PS)_8$-cyl, (B) CCS-$(PS)_8$-neu with $M_{n(PS)}$ = 2960 g/mol at different concentrations ranging from 1, 4, 7, and 10 mg/mL. (C, D) SEM images prepared from CCS-$(PS)_8$-cyl at 1 mg/mL. Scale bar is 5 μm.

Formation of Honeycomb-Patterned Porous Films via Self-assembly of Breath Figures

The breath figure method has been considered as a simple bottom-up technique for preparing honeycomb-patterned porous films. **Fig. 5** shows SEM images prepared from the end-functionalized stars CCS–$(PS)_8$–cyl and CCS–$(PS)_8$–neu in CS_2 with the concentration ranging from 1 to 10 mg/mL. It should be pointed out that the ionized star polymers are insoluble in common organic reagents because of the strong intra- and/or inter-molecular interaction although the ionized linear polymer is soluble. All of the films are large area uniform except that prepared from CCS–$(PS)_8$–cyl at 1 mg/mL, which consists of both ordered and disrupt areas (**Fig. 5A, C, D**). It can be attributed to the relatively poor ability of CCS–$(PS)_8$–cyl at low concentration to precipitate at the solution/water interface to stabilize the water droplets to prevent from coalescing. For comparison, we investigated the film-forming property of linear PS with a molecular weight of 28900 g/mol that is close to that of the star polymer (**Fig. S2**). As shown in **Fig. S3**, ordered structure can only be fabricated at 10 mg/mL for linear PS-neu. Linear PS-cyl, which has a less hydrophilic end group, forms disordered films in all studied concentration ranges. The star polymer is more likely to form ordered honeycomb films than the corresponding linear polymer because higher segment density of star polymers makes it easier to form a thin polymer layer at the solution/water interface to stabilize the condensed water droplets.[41] Our results verify this conclusion and further demonstrate that the end group of star polymers may show obvious influences on the surface uniformity of honeycomb films when the polymer concentration is relatively low.

Fig. 6 displays the top-down SEM images of honeycomb films prepared from star polymers having different arm numbers and arm length at 10 mg/mL, in which the linear component is around 10~20%. The arm number ranges from about 4 to 16 (CCS–$(PS)_N$–cyl and CCS–$(PS)_N$–neu, N = ~4, 8, 12, 16), and the molecular weight of a single arm or the macroinitiator distributes from 2960 to 5950 g/mol (CCS–$(M_{n,PS})_N$–cyl and CCS–$(M_{n,PS})_N$–neu, $M_{n,PS}$ = 2960, 4440, 5950 g/mol). It can be seen that the end-functionalized star polymers are able to form highly ordered honeycomb films apart from CCS–$(PS)_4$–neu. Overall, the pore size of the films changes little in our case. Moreover, it can also be found that star polymers with low molecular weight arms, low arm number and cyclic end groups (e.g., CCS–$(2960)_4$–cyl, CCS–$(2960)_8$–cyl, CCS–$(2960)_{12}$–cyl, and CCS–$(4440)_4$–cyl) results in micro-sized honeycomb films surrounded with nano-sized satellite pores. These satellite pores should be attributed to the uncollided water.[59]

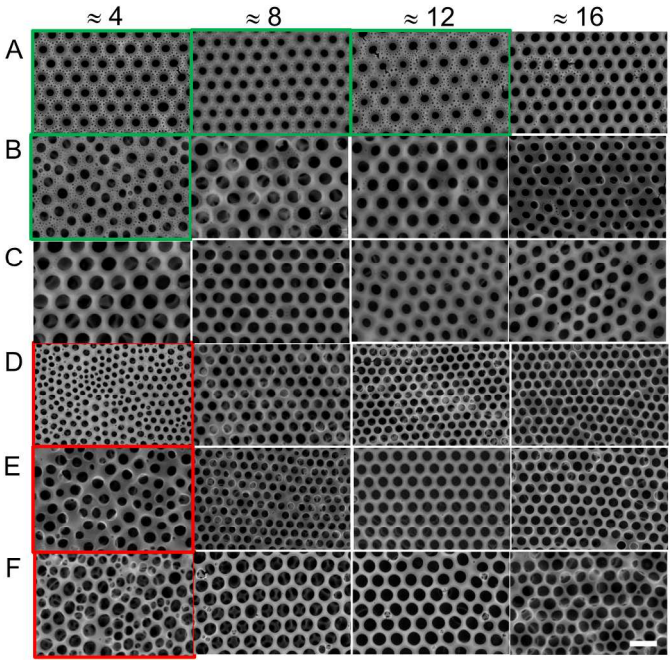

Fig. 6 Top-down SEM images of honeycomb films prepared from (A) CCS-$(2960)_N$-cyl, (B) CCS-$(4440)_N$-cyl, (C) CCS-$(5950)_N$-cyl, (D) CCS-$(2960)_N$-neu, (E) CCS-$(4440)_N$-neu, and (F) CCS-$(5950)_N$-neu with *N* ranges of about 4, 8, 12, and 16 at 10 mg/mL. The value inside the parentheses is the molecular weight of the arm. Scale bar is 5 μm.

Fig. 7 shows the cross-sectional view of the honeycomb films prepared from stars with N = 4 and 16. Before hydrolysis (top three rows), the honeycomb films fabricated from CCS–$(PS)_4$–cyl changes from monolayer (Fig 7A) to bilayer (Fig. 7B, C) with the increase of arm length; however, CCS–$(PS)_{16}$–cyl always forms mono-layered structure. After hydrolysis and acidification (bottom three rows), honeycomb films with multilayer structure were prepared from the CCS polymers with neutralized end groups and four arms, i.e., CCS–$(PS)_4$–neu. The layer number decreases to monolayer or bilayer when increasing the arm number to 16.

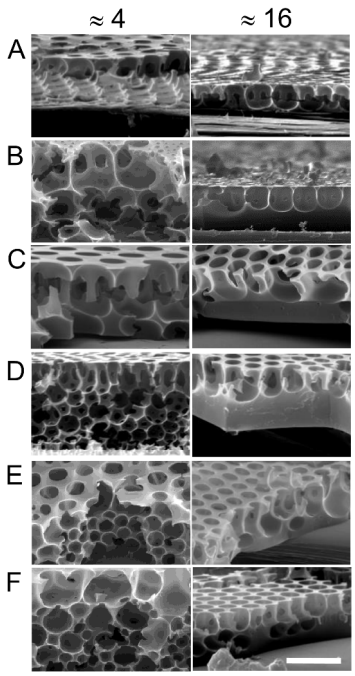

Fig. 7 Cross-section SEM images of honeycomb films prepared from (A) CCS-$(2960)_N$-cyl, (B) CCS-$(4440)_N$-cyl, (C) CCS-$(5950)_N$-cyl, (D) CCS-$(2960)_N$-neu, (E) CCS-$(4440)_N$-neu, and (F) CCS-$(5950)_N$-neu with $N \approx 4$ and 16 at 10 mg/mL. The value inside the parentheses is the molecular weight of the arm. Scale bar is 5 μm.

It is well known that the viscosity of polymer solution might affect the film structure. The solution for film formation has a very low initial concentration of around 1%, at which the viscosity changes little for these star polymers with different arm length or arm numbers. However, the solution will concentrate continuously with the evaporation of solvent, and then the viscosity may act as a prominent factor influencing the multilayer structure. Higher viscosity can weaken solvent evaporation[60] and hence afford longer solidification time during which condensed water droplets will more probably sink into the bottom of the solution, facilitating the formation of bilayer or multilayer structure. On the other hand, the sinking of encapsulated water droplets can be slowed down in high viscosity solution.[7] Fetters et al. demonstrated that the viscosity increases with the arm length while maintaining the equivalent arm number and increases with the arm number for fixed arm length.[61] As shown in the top three rows of **Fig. 7**, bilayer structure is more likely to be obtained from polymers with longer arm length that have relatively high solution viscosity, i.e. CCS–$(4440)_4$–cyl and CCS–$(5950)_4$–cyl. On contrast, stars having higher arm number (N = 16) form monolayer film although they have higher viscosity. Therefore, it seems that the solution viscosity shows two entirely different impacts on the film structure. As we know, the segment density of the stars may be another influence. However, the exact mechanism still needs further investigation.

Notably, honeycomb films with multilayer structure have been prepared from star polymers with hydrophilic end groups, i.e. CCS–$(PS)_4$–neu. The hydrophilic end groups can help to stabilize the condensed water droplets via segregating at the solution/water interface.[62] As polymers with hydrophilic end groups possess strong interfacial activity,[63-64] it is speculated that the sinking process of water droplets may be induced by faster stabilization and elongated solidifying processes. Therefore, the stars with hydrophilic end groups tend to form multilayer structures. We can also see that bilayer structure have been obtained even for stars with 16 arms (CCS-$(4440)_{16}$-neu and CCS-$(5950)_{16}$-neu).

Conclusions

Core cross-linked star polystyrenes with relatively hydrophobic and hydrophilic end groups have been synthesized via the "arm-first" approach using a linear polystyrene macroinitiator, which is end-functionalized with a hydrolysable cyclic group. The cyclic lactone end group was converted to neutralized groups by alkaline hydrolysis and acidification processes. The star polymers are easier to form ordered honeycomb films than the corresponding linear analogue because of the higher segment density of stars. Moreover, the end groups of the stars show impact on the film surface structures, especially film uniformity, only at relatively low concentration. More importantly, stars with lower arm numbers or longer arms tend to form bilayer or multilayer structured films. On the other hand, stars with hydrophilic end groups are much easier to form bilayer or multilayer structured films because of the improved interfacial activity.

Acknowledgements

This work is supported by the National Natural Science Foundation of China (21374100 and 51173161).

Notes and references

MOE Key Laboratory of Macromolecular Synthesis and Functionalization, Department of Polymer Science and Engineering, Zhejiang University, Hangzhou 310027, China. E-mail: lswan@zju.edu.cn. Phone: +86-571-87953763.

Electronic Supplementary Information (ESI) available: [Detailed information regarding the synthesis of end-functionalized linear polystyrene; fitted GPC curves of CCS-$(PS)_4$-cyl; GPC curve of linear PS-cyl; SEM images prepared from linear polymer]. See DOI: 10.1039/c000000x/

1. G. Widawski, M. Rawiso and B. Francois, *Nature* 1994, **369**, 387-389.
2. M. Srinivasarao, D. Collings, A. Philips and S. Patel, *Science* 2001, **292**, 79-83.
3. U. H. F. Bunz, *Adv. Mater.* 2006, **18**, 973-989.
4. J. Jin, L. S. Wan, B. B. Ke and Z. K. Xu, *Prog. Chem.* 2010, **22**, 2173-2178.
5. H. M. Ma and J. C. Hao, *Chem. Soc. Rev.* 2011, **40**, 5457-5471.
6. L. J. Xue, J. L. Zhang and Y. C. Han, *Prog. Polym. Sci.* 2012, **37**, 564-594.
7. M. Hernandez-Guerrero and M. H. Stenzel, *Polym. Chem.* 2012, **3**, 563-577.
8. P. Escale, L. Rubatat, L. Billon and M. Save, *Eur. Polym. J.* 2012, **48**, 1001-1025.
9. H. Bai, C. Du, A. J. Zhang and L. Li, *Angew. Chem. Int. Ed.* 2013, **52**, 12240-12255.
10. A. Munoz-Bonilla, M. Fernández-García and J. Rodríguez-Hernández, *Prog. Polym. Sci.* 2014, **39**, 510-554.

11. L. S. Wan, L. W. Zhu,Y. Ou and Z. K. Xu, *Chem. Commun.* 2014, **50**, 4024-4039.
12. H. Yabu, R. Jia, Y. Matsuo, K. Ijiro, S. Yamamoto, F. Nishino, T. Takaki, M. Kuwahara and M. Shimomura, *Adv. Mater.* 2008, **20**, 4200-4204.
13. H. Meng, L. Y. Liu and W. T. Yang, *Chin. J. Polym. Sci.* 2009, **27**, 903-908.
14. Y. Hirai, H. Yabu, Y. Matsuo, K. Ijiro and M. Shimomura, *Chem. Commun.* 2010, **46**, 2298-2300.
15. C. Y. Ma, Y. W. Zhong, J. Li, C. K. Chen, J. L. Gong, S. Y. Xie, L. Li and Z. Ma, *Chem. Mater.* 2010, **22**, 2367-2374.
16. S. H. Lee, H. W. Kim, J. O. Hwang, W. J. Lee, J. Kwon, C. W. Bielawski, R. S. Ruoff and S. O. Kim, *Angew. Chem. Int. Ed.* 2010, **49**, 10084-10088.
17. L. S. Wan, J. Lv, B. B. Ke and Z. K. Xu, *ACS Appl. Mater. Interfaces* 2010, **2**, 3759-3765.
18. B. B. Ke, L. S. Wan and Z. K. Xu, *Langmuir* 2010, **26**, 8946-8952.
19. W. Sun, L. Y. Shen, J. M. Wang, K. Fu and J. Ji, *Langmuir* 2010, **26**, 14236-14240.
20. J. Wang, C. F. Wang, H. X. Shen and S. Chen, *Chem. Commun.* 2010, **46**, 7376-7378.
21. B. B. Ke, L. S. Wan, P. C. Chen, L. Y. Zhang and Z. K. Xu, *Langmuir* 2010, **26**, 15982-15988.
22. H. M. Ma, J. W. Cui, J. F. Chen and J. C. Hao, *Chem. Eur. J.* 2011, **17**, 655-660.
23. W. X. Zhang, L. S. Wan, X. L. Meng, J. W. Li, B. B. Ke, P. C. Chen and Z. K. Xu, *Soft Matter* 2011, **7**, 4221-4227.
24. B. B. Ke, L. S. Wan, Y. Li, M. Y. Xu and Z. K. Xu, *Phys. Chem. Chem. Phys.* 2011, **13**, 4881-4887.
25. P. C. Chen, L. S. Wan, B. B. Ke and Z. K. Xu, *Langmuir* 2011, **27**, 12597-12605.
26. L. S. Wan, J. W. Li, B. B. Ke and Z. K. Xu, *J. Am. Chem. Soc.* 2012, **134**, 95-98.
27. J. Z. Chen, X. Z. Yan, Q. L. Zhao, L. Li and F. H. Huang, *Polym. Chem.* 2012, **3**, 458-462.
28. Y. Y. Ma, J. Liang, H. Sun, L. X. Wu, Y. Q. Dang and Y. Q. Wu, *Chem. Eur. J.* 2012, **18**, 526-531.
29. L. S. Wan, Q. L. Li, P. C. Chen and Z. K. Xu, *Chem. Commun.* 2012, **48**, 4417-4419.
30. C. Deleuze, C. Derail, M. H. Delville and L. Billon, *Soft Matter* 2012, **8**, 8559-8562.
31. L. P. Heng, W. Qin, S. J. Chen, R. R. Hu, J. Li, N. Zhao, S. T. Wang, B. Z. Tang and L. Jiang, *J. Mater. Chem.* 2012, **22**, 15869-15873.
32. H. L. Cong, J. L. Wang, B. Yu and J. G. Tang, *Soft Matter* 2012, **8**, 8835-8839.
33. X. Xu, L. P. Heng, X. J. Zhao, J. Ma, L. Lin and L. Jiang, *J. Mater. Chem.* 2012, **22**, 10883-10888.
34. Y. Xue, H. C. Lu, Q. L. Zhao, J. Huang, S. G. Xu, S. K. Cao and Z. Ma, *Polym. Chem.* 2013, **4**, 307-312.
35. M. V. Walter, P. Lundberg, D. Hult, A. Hult and M. Malkoch, *Polym. Chem.* 2013, **4**, 2680-2690.
36. A. S. de Leon, A. del Campo, C. Labrugere, M. Fernandez-Garcia, A. Munoz-Bonilla and J. Rodriguez-Hernandez, *Polym. Chem.* 2013, **4**, 4024-4032.
37. P. Escale, W. Van Camp, F. Du Prez, L. Rubatat, L. Billon and M. Save, *Polym. Chem.* 2013, **4**, 4710-4717.
38. L. P. Heng, R. R. Hu, S. J. Chen, M. C. Li, L. Jiang and B. Z. Tang, *Langmuir* 2013, **29**, 14947-14953.
39. X. Y. Zhou, Z. H. Chen, Y. Z. Wang, Y. Guo, C. H. Tung, F. S. Zhang and X. W. Liu, *Chem. Commun.* 2013, **49**, 10614-10616.
40. Y. Ou, L. W. Zhu, W. D. Xiao, H. C. Yang, Q. J. Jiang, X. Li, J. G. Lu, L. S. Wan, Z. K. Xu, *J. Phys. Chem. C* 2014, **118**, 4403-4409.
41. O. Pitois and B. Francois, *Eur. Phys. J. B* 1999, **8**, 225-231.
42. M. H. Stenzel-Rosenbaum, T. P. Davis, A. G. Fane and V. Chen, *Angew. Chem. Int. Ed.* 2001, **40**, 3428-3432.
43. C. Barner-Kowollik, H. Dalton, T. P. Davis and M. H. Stenzel, *Angew. Chem. Int. Ed.* 2003, **42**, 3664-3668.
44. L. A. Connal and G. G. Qiao, *Adv. Mater.* 2006, **18**, 3024-3028.
45. L. A. Connal, R. Vestberg, P. A. Gurr, C. J. Hawker and G. G. Qiao, *Langmuir* 2008, **24**, 556-562.
46. L. A. Connal, R. Vestberg, C. J. Hawker and G. G. Qiao, *Adv. Funct. Mater.* 2008, **18**, 3706-3714.
47. J. C. Hsu, K. Sugiyama, Y. C. Chiu, A. Hirao and W. C. Chen, *Macromolecules* 2010, **43**, 7151-7158.
48. Z. Zhang, T. C. Hughes, P. A. Gurr, A. Blencowe, X. Hao and G. G. Qiao, *Adv. Mater.* 2012, **24**, 4327-4330.
49. L. W. Zhu, L. S. Wan, J. Jin and Z. K. Xu, *J. Phys. Chem. C* 2013, **117**, 6185-6194.
50. L. W. Zhu, W. Yang, Y. Ou, L. S. Wan, and Z. K. Xu, *Polym. Chem.* 2014, **5**, 3666-3672.
51. L. S. Wan, B. B. Ke, X. K. Li, X. L. Meng, L. Y. Zhang and Z. K. Xu, *Sci. China Series B-Chem.* 2009, **52**, 969-974.
52. J. H. Xia, X. Zhang and K. Matyjaszewski, *Macromolecules* 1999, **32**, 4482-4484.
53. A. W. Jackson, C. Stakes and D. A. Fulton, *Polym. Chem.* 2011, **2**, 2500-2511.
54. J. Zeng, P. C. Du and P. Liu, *RSC Adv.* 2013, **3**, 19492-19500.
55. Q. J. Chen, Y. Y. Xu, X. T. Cao, L. J. Qin and Z. S. An, *Polym. Chem.* 2014, **5**, 175-185.
56. A. Blencowe, J. F. Tan, T. K. Coh and G. G. Qiao, *Polymer* 2009, **50**, 5-32.
57. J. D. Zeng, J. Zhu, X. Q. Pan, Z. B. Zhang, N. C. Zhou, Z. P. Cheng, W. Zhang and X. L. Zhu, *Polym. Chem.* 2013, **4**, 3453-3457.
58. X. L. Miao, W. Zhu, Z. B. Zhang, W. Zhang, X. L. Zhu and J. Zhu, *Polym. Chem.* 2014, **5**, 551-557.
59. L. Li, C. K. Chen, J. Li, A. J. Zhang, X. Y. Liu, B. Xu, S. B. Gao, G. H. Jin and Z. Ma, *J. Mater. Chem.* 2009, **19**, 2789-2796.
60. Y. Xu, B. K. Zhu and Y. Y. Xu, *Polymer* 2005, **46**, 713-717.
61. L. J. Fetters, A. D. Kiss, D. S. Pearson, G. F. Quack and F. J. Vitus, *Macromolecules* 1993, **26**, 647-654.
62. M. H. Stenzel, C. Barner-Kowollik and T. P. Davis, *J. Polym. Sci. Part A: Polym. Chem.* 2006, **44**, 2363-2375.
63. L. W. Zhu, Y. Ou, L. S. Wan and Z. K. Xu, *J. Phys. Chem. B* 2014, **118**, 845-854.
64. L. W. Zhu, B. H. Wu, L. S. Wan and Z. K. Xu, *Polym. Chem.* 2014, DOI: 10.1039/C4PY00206G.

Graphical Abstract

Synthesis of Core Cross-linked Star Polystyrene with Functional End Groups and the Self-assemblies Templated by Breath Figures

Liang-Wei Zhu, Wu Yang, Ling-Shu Wan* and Zhi-Kang Xu

MOE Key Laboratory of Macromolecular Synthesis and Functionalization, Department of Polymer Science and Engineering, Zhejiang University, Hangzhou 310027, China.

E-mail: lswan@zju.edu.cn. Phone: +86-571-87953763.

We report the synthesis of core cross-linked star (CCS) polymers with functional end groups for self-assembled films, which show mono-layer and multi-layer transition, depending on arm numbers, arm length, and the end groups.